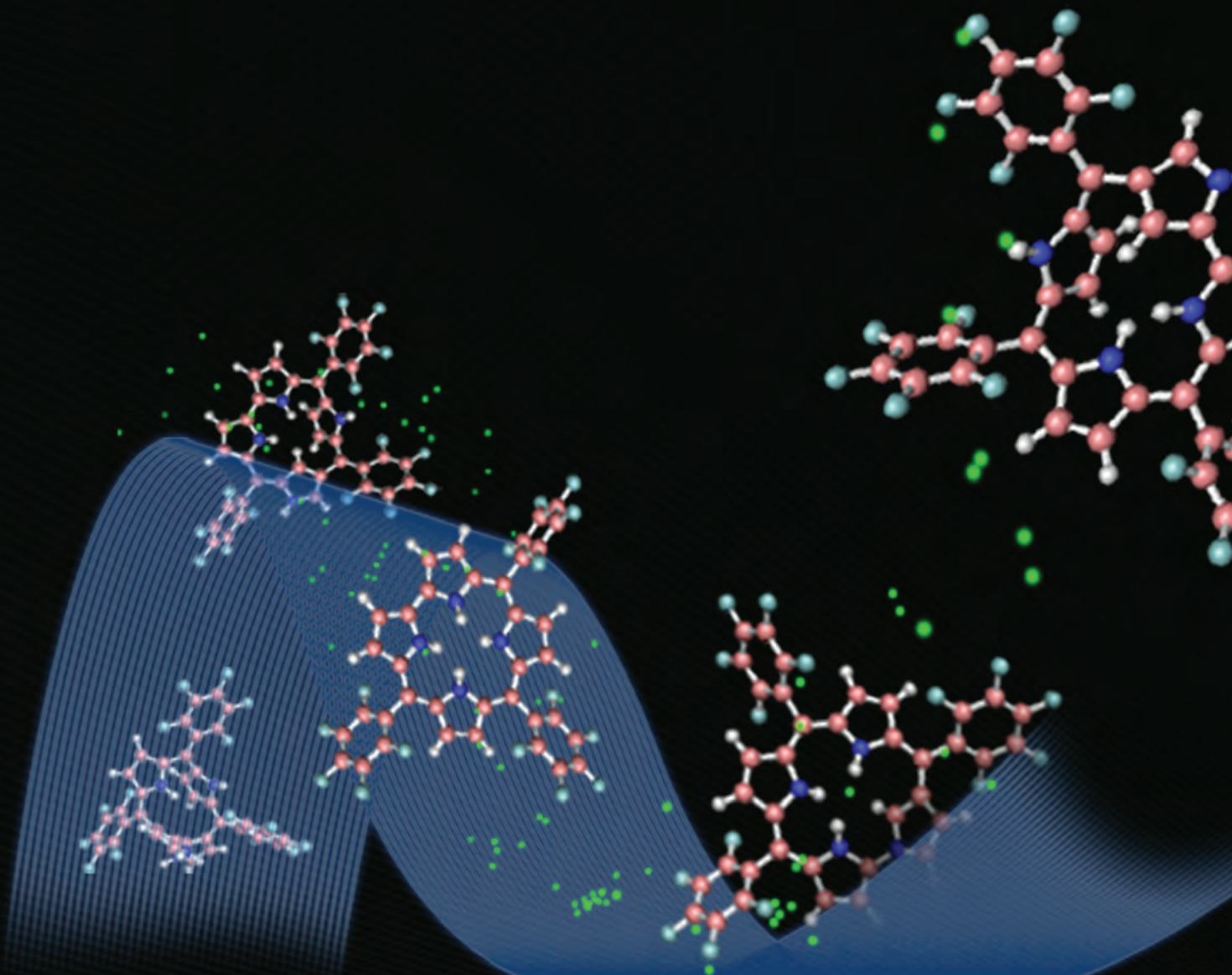


# Organic & Biomolecular Chemistry

[www.rsc.org/obc](http://www.rsc.org/obc)

Volume 10 | Number 42 | 14 November 2012 | Pages 8373–8552

Published on 28 August 2012. Downloaded by UNIVERSIDAD ESTADUAL DE CAMPINAS on 02/07/2015 14:47:12.

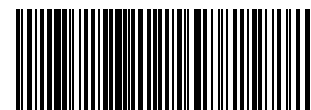


ISSN 1477-0520

RSC Publishing

**PAPER**

Hiroyuki Furuta, Koiti Araki, Marcos N. Eberlin *et al.*  
Corrole isomers: intrinsic gas-phase shapes *via* traveling wave ion mobility mass spectrometry and dissociation chemistries *via* tandem mass spectrometry



1477-0520 (2012) 10: 42; 1-9

Cite this: *Org. Biomol. Chem.*, 2012, **10**, 8396

www.rsc.org/obc

PAPER

## Corrole isomers: intrinsic gas-phase shapes *via* traveling wave ion mobility mass spectrometry and dissociation chemistries *via* tandem mass spectrometry†

Maíra Fasciotti,<sup>a,b</sup> Alexandre F. Gomes,<sup>c</sup> Fabio C. Gozzo,<sup>c</sup> Bernardo A. Iglesias,<sup>d</sup> Gilberto F. de Sá,<sup>e</sup> Romeu J. Daroda,<sup>f</sup> Motoki Toganoh,<sup>g</sup> Hiroyuki Furuta,<sup>\*g</sup> Koiti Araki<sup>\*d</sup> and Marcos N. Eberlin<sup>\*a</sup>

Received 25th June 2012, Accepted 24th August 2012

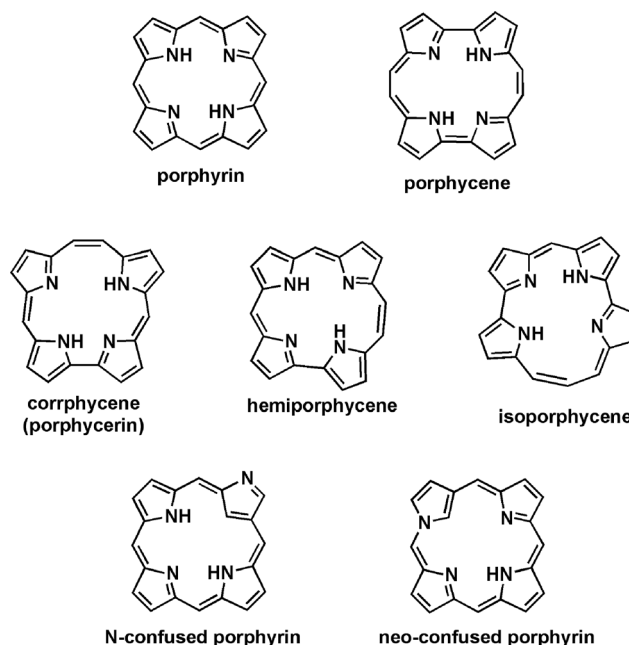
DOI: 10.1039/c2ob26209f

Corrole and four of its isomers with subtle structural changes promoted by exchange of nitrogen and carbon atoms in the corrole ring have been studied by traveling wave ion mobility mass spectrometry and collision induced dissociation experiments. Significant differences in shapes and charge distributions for their protonated molecules were found to lead to contrasting gas phase mobilities, most particularly for corrorin, the most “confused” isomer. Accordingly, corrorin was predicted by B3LYP/6-31g(d,p) and collisional cross section calculations to display the most compact tri-dimensional structure, whereas NCC4 and corrole were found to be the most planar isomers. Better resolution between the corrole isomers was achieved using the more polarizable and massive CO<sub>2</sub> as the drift gas. Sequential losses of HF molecules were found to dominate the dissociation chemistry of the protonated molecules of these corrole isomers, but their unique structures caused contrasting labilities towards CID, whereas NCC4 showed a peculiar and structurally diagnostic loss of NH<sub>3</sub>, allowing its prompt differentiation from the other isomers.

### Introduction

Most of the beauty and diversity of molecules comes from isomerism and the innumerable possibilities of arrangements of a given set of atoms in multiform chains, branches and rings in the three-dimensional space. Characterization, identification and the measurement of the distinctive physico-chemical properties of isomeric molecules are therefore a subject of fundamental importance in chemistry. For porphyrins, a multitude of isomers with peculiar properties have been generated by changing the number of carbon atoms between pyrrole rings such as in porphycenes,<sup>1</sup>

porphycerins,<sup>2,3</sup> hemiporphycenes,<sup>4</sup> and isoporphycenes<sup>5</sup> (Scheme 1). Exceptional examples of porphyrin isomers are



Scheme 1 Structures of porphyrin and porphyrinoid isomers.

<sup>a</sup>ThoMson Mass Spectrometry Laboratory, Institute of Chemistry, University of Campinas – UNICAMP, 13084-970 Campinas, SP, Brazil. E-mail: eberlin@iqm.unicamp.br

<sup>b</sup>Institute of Chemistry, University of Campinas – UNICAMP, 13084-862 Campinas, SP, Brazil

<sup>c</sup>Dalton Mass Spectrometry Laboratory, University of Campinas – UNICAMP, Brazil

<sup>d</sup>Institute of Chemistry, University of Sao Paulo, Av. Prof. Lineu Prestes 748, CEP 05508-000, São Paulo, SP, Brazil

<sup>e</sup>Department of Fundamental Chemistry, Federal University of Pernambuco, 50.740-540 Recife, PE, Brazil

<sup>f</sup>National Institute of Metrology, Standardization and Industrial Quality, Division of Chemical Metrology, 25250-020 Duque de Caxias, RJ, Brazil

<sup>g</sup>Kyushu University, Fukuoka 819-0395, JP, Japan

†Electronic supplementary information (ESI) available. See DOI: 10.1039/c2ob26209f

derived from “confusion” and “neo-confusion”, where the new structures are generated by changing the position of the nitrogen atom.<sup>6–8</sup> Because regular porphyrins have highly symmetric structures, intrinsically there is only a single isomer in N-confused porphyrin. This situation is drastically changed in asymmetric porphyrinoids such as corroles and hexaphyrins.<sup>9</sup>

The chemistry of corroles is now well developed, and the increasing number of new molecules in this class is opening their way to potential applications, in analogy with porphyrin derivatives.<sup>10</sup> There are two main routes for the preparation of *meso*-substituted corroles.

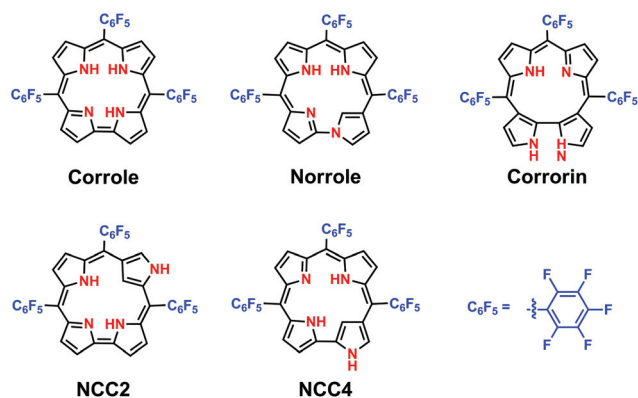
The “one pot” method is theoretically the simplest one to access A<sub>3</sub>-corrole-type compounds.<sup>11</sup> This method is however efficient only when the aldehyde is activated by electron withdrawing groups. The “2 + 1” method forms A<sub>3</sub>- and *trans*-A<sub>2</sub>B-corroles<sup>12</sup> but requires the use of encumbered dipyrromethanes to avoid the acidolysis reaction, being convenient to prepare mono-, di- and tri-*meso*-substituted corrole macrocycles. Corroles and N-confused corroles belong to a new class of contracted porphyrins that have received much recent attention, especially due to their metal coordination chemistry, spectroscopic and spectroelectrochemical properties, whose behaviors were shown to be completely different from those of their porphyrin analogues.<sup>13</sup>

Electrospray ionization mass spectrometry (ESI-MS) has been established as the gold-standard technique for the characterization of labile compounds and polar or ionic macrocycle species, such as many porphyrin and porphyrin-like derivatives.<sup>14</sup> Single stage ESI-MS is inherently unable to distinguish isomers such that strategies based on the correlation between structure and dissociation chemistry *via* tandem ESI-MS/MS experiments have therefore been used to recognize gaseous isomeric ions.<sup>15</sup> In fact, ESI-MS and ESI-MS/MS<sup>16</sup> performed with a series of metallocorroles revealed that multi-step deprotonation and oxidation processes are associated with the oxidation of the metal center, thus showing a complex ionization mechanism.

A powerful tool for the isomeric characterization is provided by the coupling of MS to ion mobility spectrometry (IMS). Isomeric ions are separated by IMS-MS while migrating through a buffer gas with a drift velocity that will depend on the charge, shape (collision cross-section, CCS) and polarity.<sup>17</sup> IMS has been mainly used to analyze compounds such as drugs, chemical warfare agents, explosives, environmental pollutants, dendrimeric and polymeric structures, as well as proteins and peptides,<sup>18,19</sup> providing invaluable information about their conformation in the native solution environment.<sup>20</sup>

Traveling wave ion mobility (TWIM) has been introduced more recently as a new mode of ion propulsion for IMS experiments.<sup>21</sup> Briefly, in TWIM ions are accumulated and periodically released into a stacked-ring ion guide (T-wave cell), where they drift under the action of a continuous train of transient voltage pulses (traveling waves) applied to pairs of stacked ring electrodes, encompassing a very compact (18.5 cm long) but efficient ion mobility cell.

Most recently, we explored the TWIM-MS technique for analyses of mixtures of *meta/para* and *cis/trans* cationic ruthenated *meso*-pyridylporphyrins<sup>22</sup> and the formation and resolution of *meso*-tetra(4- and 3-pyridyl) porphyrin protomers.<sup>23</sup> The presence of [Ru(bpy)<sub>2</sub>Cl]<sup>+</sup> complex bonds at *meta*- or *para*-pyridyl, or *cis*- or *trans*-positions leads to huge changes in the CCS and



**Scheme 2** Structures of the *meso*-pentafluorophenyl N-confused corrole isomers.

dipolar moments. However, the changes become more subtle when the ruthenium complex is substituted by H<sup>+</sup>, but the basicity of the pyridyl group and porphyrin ring N-atoms as well as the electrostatic contribution due to the formation of the biprotonated species were comparatively evaluated. In this case, a singly inner ring protonated porphyrin species and a doubly protonated species at the porphyrin ring and one peripheral pyridyl group were characterized in the gas phase for the first time.

Recently, novel *meso*-pentafluorophenyl N-confused corrole isomers<sup>24</sup> (NCC2, NCC4, norrole and corrorin,<sup>25</sup> Scheme 2) were successfully synthesized inspiring us to examine their gas phase behavior by TWIM-MS. These isomeric macrocyclic molecules are relatively small and structurally very similar, posing quite a challenge to distinguish them. Furthermore, TWIM-MS analyses of those corrole isomers will shed light on their gas-phase behavior as well as interaction with small polarizable gas molecules such as N<sub>2</sub> and CO<sub>2</sub>. Such information would be of relevance for the understanding of the chemistry of N-confused corroles.<sup>26</sup>

## Results and discussion

### TWIM-MS analysis

The relative gas phase mobilities of the five corrole isomers (Scheme 2) were first evaluated by TWIM-MS using ESI in the positive ion mode. Fundamentally, the ion mobility in TWIM experiments is related to the time that a packet of ions takes to travel through a gas-filled, stacked-ring ion guide under the influence of a pulsed electric field. This drift time depends on several parameters such as temperature, pressure, molecular weight and polarizability of the drift gas, as well as ion charge distribution and CCS that depends on the interaction of a given ion with the neutral gas molecules. It also is influenced by the velocity and height of the traveling wave pulse applied at the T-wave cell.<sup>27</sup>

Metrics similar to those used in chromatography can also be calculated for ion mobility experiments to evaluate the resolution amongst two adjacent isomers. The first parameter is the separation factor ( $\alpha$ ), which is the ratio between the drift times of two adjacent peaks (eqn (1)).

$$\alpha = \frac{dt_b}{dt_a} \quad (1)$$



The resolving power ( $R_p$ ) of the technique is dependent on single-peak resolution parameters, *i.e.* the ratio between the drift time ( $dt$ ) and the peak width at half height ( $w_{1/2}$ ), according to eqn (2).

$$R_p = \frac{dt}{w_{1/2}} \quad (2)$$

$R_p$  can be related to peak-to-peak resolution ( $R_{p-p}$ ) by eqn (3), which indicates a linear correlation between the separation of two adjacent peaks and the product of  $\alpha - 1$  and  $R_p$ .<sup>28</sup>

$$R_{p-p} = 0.589 R_p \frac{\alpha - 1}{\alpha} \quad (3)$$

Those parameters are highly affected by the nature of the drift gas and its pressure. Generally, increasing the drift gas pressure results in higher mobility resolution. Whereas nitrogen is the default drift gas in commercial TWIM instruments, more polarizable gases such as  $\text{CO}_2$  can improve the mobility separation.<sup>29</sup> The ion mobilities of isomeric corroles and N-confused analogues were therefore evaluated with  $\text{N}_2$  and  $\text{CO}_2$ , whose polarizability volumes are  $1.7403 \times 10^{-24}$  and  $2.9110 \times 10^{-24} \text{ cm}^3$ , respectively. When using the more massive  $\text{CO}_2$ , however, a lower pressure was used to avoid excessive loss of sensitivity. Before analyzing the isomeric mixtures and to evaluate the respective ion mobility parameters, TWIM-MS experiments were performed with each one of the protonated corrole isomers ( $[\text{M} + \text{H}]^+$ ) formed *via* ESI(+). Fig. 1 shows the results as overlaid drift time plots.

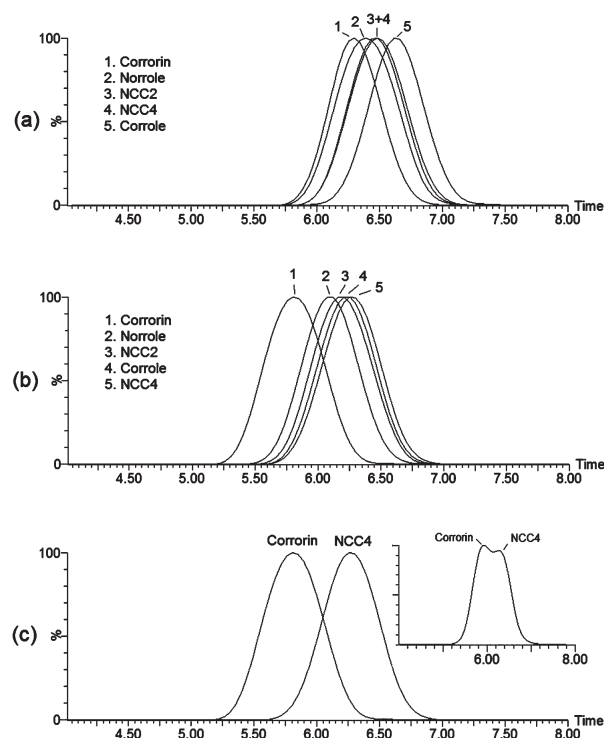
Table 1 shows the  $R_p$  values, evaluated for the five isomers from the drift time plots of Fig. 1 using eqn (2).  $R_p$  should be a constant for a given TWIM experimental condition, but varied slightly for a set of analyses due to fluctuations in drift time and  $w_{1/2}$ . Accordingly, Table 1 lists the more significant averages. Note that the  $R_p$  values determined for all five molecules, except norrole, were slightly lower in  $\text{CO}_2$  rather than in  $\text{N}_2$  as the drift gas, likely due to the higher  $\text{N}_2$  pressures and lower wave velocities ( $250 \text{ m s}^{-1}$ ) in  $\text{CO}_2$ .

Fig. 1a shows the TWIM-MS data for pure samples of the corrole isomers using  $\text{N}_2$  as the drift gas. Corrorin was the isomer with the higher mobility (6.30 ms), followed by norrole (6.34 ms), NCC2 and NCC4 showing nearly the same drift time (6.48 ms), and finally corrole (6.61 ms).

Table 2 lists for each isomer the separation factor ( $\alpha$ ) and peak-to-peak resolution ( $R_{p-p}$ ) in  $\text{N}_2$  and  $\text{CO}_2$ .

Despite the comparable  $R_p$  in  $\text{N}_2$  and  $\text{CO}_2$ , significantly greater  $R_{p-p}$  was generally achieved with  $\text{CO}_2$ , even though a lower drift gas pressure (1.00 mbar) was used. This result shows that the drift gas mass, or its polarizability, has a pronounced influence on the mobility of those corrole isomers suggesting that the charge distribution on the ion plays a fundamental role perhaps by changing the ion–dipole interactions with the neutral gas. In fact, the isomeric pairs corrole/corrorin, NCC4/corrorin, norrole/corrorin and NCC2/corrorin have shown the best  $R_{p-p}$  in  $\text{CO}_2$  (values in bold in Table 2).

Despite the small differences in drift times, there are significant differences in the ion mobility when the positions of N and C atoms are exchanged in the corrole core thus allowing their distinction by TWIM-MS. Note that we have used the 1st



**Fig. 1** Overlaid drift time plots obtained for the protonated molecules of separately analyzed corrole, corrorin, norrole, NCC2 and NCC4. Methanolic solutions of pure samples were used. General conditions were: (a)  $\text{N}_2$  pressure = 2.00 mbar, wave velocity =  $250 \text{ m s}^{-1}$  and wave height = 30.0 V; (b)  $\text{CO}_2$  pressure = 1.00 mbar, wave velocity =  $280 \text{ m s}^{-1}$  and wave height = 30.0 V; and (c) overlaid drift time plots for corrorin and NCC4 using the (b) settings. The inset in (c) shows the drift time plot for a mixture of corrorin and NCC4 under the same experimental conditions.

**Table 1** Resolving power ( $R_p$ ) using  $\text{N}_2$  and  $\text{CO}_2$

Isomer	Resolving power ( $R_p$ )	
	$\text{N}_2$	$\text{CO}_2$
Corrole	13.50	11.39
Corrorin	13.76	10.10
Norrole	11.26	12.62
NCC2	12.73	11.90
NCC4	12.50	11.92
Average $R_p$	12.73	11.90

generation lower resolution TWIM cell, hence much improved resolution is expected for the 2nd generation G2 cell with 4 times greater  $R_p$ .<sup>30</sup> These differences mean that there are significant changes in the CCS, dipole moment and/or polarizability of these isomeric species to influence the gaseous ion–drift gas interactions and, consequently, the drift times.

If CCS plays indeed a major factor influencing the drift times of these isomers, the TWIM-MS plots would indicate that corrorin should have the most compact and corrole the less compact structure, whereas NCC2, NCC4 and norrole (“NCC isomers”) should exhibit intermediate CCS values between corrole and corrorin.

**Table 2** Separation factor ( $\alpha$ ) and peak-to-peak resolution ( $R_{p-p}$ ) calculated for each pair of isomers using  $N_2$  and  $CO_2$  as the drift gas

Isomeric pairs	$N_2$		$CO_2$	
	$\alpha$	$R_{p-p}$	$\alpha$	$R_{p-p}$
Corrole/corrorin	1.05	0.35	1.07	<b>0.46</b>
NCC4/NCC2	1.00	0.00	1.01	0.06
NCC2/norrole	1.02	0.16	1.01	0.10
NCC4/norrole	1.02	0.16	1.02	0.16
Corrole/norrole	1.04	0.31	1.01	0.10
NCC4/corrorin	1.03	0.21	1.08	<b>0.52</b>
Norrole/corrorin	1.01	0.05	1.06	<b>0.37</b>
Corrole/NCC2	1.02	0.15	1.00	0.00
Corrole/NCC4	1.02	0.15	1.01	0.06
NCC2/corrorin	1.03	0.21	1.07	<b>0.46</b>

A similar behavior and tendency is observed using  $CO_2$  as the drift gas (Fig. 1b), but in  $CO_2$  corrorin shows a much distinctive mobility being by far the fastest among all isomers. Such a higher difference in the drift times led to a reasonable  $R_{p-p}$  of *ca.* 0.5 in the 1st generation cell for the NCC4/corrorin pair (Fig. 1c and Table 2).

### Theoretical calculations

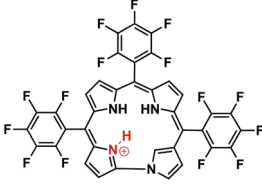
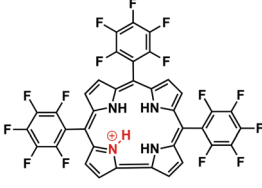
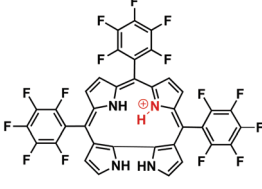
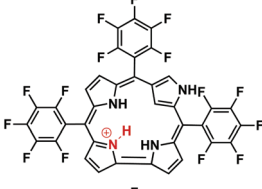
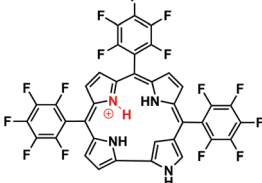
Some relevant parameters of the corrole isomers, intimately related to the ion mobility in the gas phase, were estimated by molecular modelling and used to rationalize the experimental TWIM-MS results. We first determined the most probable protonated sites for each isomeric species by comparing the electronic energies calculated at the B3LYP/6-31g(d,p) level for protonation at any of the four core nitrogen atoms. As compared to the neutral molecules, protonation was found to have little if any influence on the final optimized structures.

Protonation of a nitrogen on 2*H*-pyrrole-like rings (imines) was shown to be favored as compared to 1*H*-pyrrole-like rings (amines). After determining the most stable protonated molecule, their CCS values were calculated using the trajectory method (TM) implemented in the MOBCAL software (Table 3).

Typically, the mobility of an ion is exclusively dependent on its CCS when He is used as the drift gas, because irrelevant ion-dipole interaction occurs between the ion and He. It is known, however, that when polarizable drift gases are used, significant ion-induced dipole interactions affect mobility by creating interaction potentials between the ion and the neutral collision partners driven by the chemical nature of the analyte.<sup>31</sup> This interaction may be traduced by the charge dispersion on the gaseous ions that will result in different magnitudes of the ion-dipole and dipole-dipole interactions and lifetimes for the ion-molecule complexes formed with the drift gas.<sup>34</sup> To have an estimation of these crucial interactions, the dipole moments of the most stable protonated molecules were therefore calculated. Table 3 summarizes all calculated parameters involved in TWIM separations (for all the calculation results see ESI†).

Surprisingly due to the quite contrasting levels of “N-confusion” for the five isomers, the calculations (Table 3) predict very similar CCS, from 209.27 Å<sup>2</sup> for norrole to 212.23 Å<sup>2</sup> for NCC2. The CCS window is therefore less than 3 Å<sup>2</sup>, that is,

**Table 3** CCS values (MOBCAL TM method) and dipole moments of corrole isomers calculated at the B3LYP/6-31g(d,p) level using Gaussian03

Isomer	Most favorable protonated species <sup>a</sup>	$\Omega_{He}$ (Å <sup>2</sup> )	Dipole moment (D)
Norrole		209.27	4.95
Corrole		210.77	5.15
Corrorin		209.78	2.64
NCC2		212.23	6.32
NCC4		210.11	7.03

<sup>a</sup> As estimated by electronic energies determined at the B3LYP/6-31g(d,p) level (see ESI†).

~1.5%. CCS for norrole (209.27 Å<sup>2</sup>) is found to be almost identical (0.24%) to that of corrorin (209.78 Å<sup>2</sup>). The five isomers display therefore somewhat contrasting shapes (Fig. 2) but overall very similar intrinsic CCS and in He and  $N_2$  (Fig. 1a) drift times should be quite close. Note also the same trend should apply to the neutral gaseous molecules since protonation has been found to have little if any influence in the final optimized structures. More polarizable drift gases such as  $CO_2$  should form, however, ion-molecule complexes with considerably long lifetimes and a broader drift time window may therefore be obtained. These lifetimes are expected to increase as a function of the ion's dipole moment.

For instance, protonated corrorin displays a theoretical CCS which is less than 1% larger than that of protonated NCC4 (Table 3), but the observation of a considerably shorter drift time for corrorin in  $CO_2$  (Fig. 1) can be explained considering that its

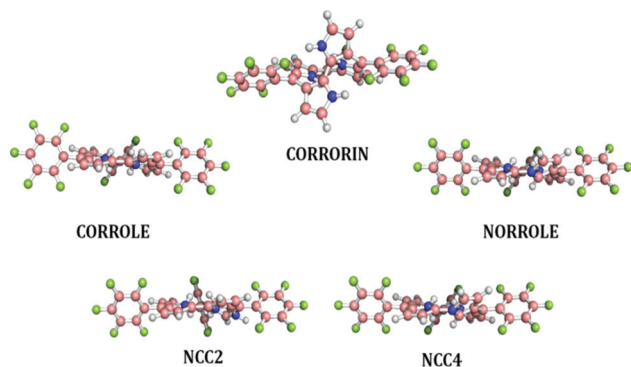
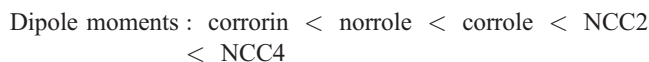


**Fig. 2** Optimized geometries at the B3LYP/6-31g(d,p) level of all five corrole isomers in their protonated forms. Figures were generated using PyMOL v.1.4 software.<sup>32</sup>

dipole moment (2.64 D) is about 1/3 that of NCC4 (7.03 D). Note the nearly perfect agreement between the drift time order in CO<sub>2</sub> and dipole moments:



In short, theoretical calculations for all five corrole isomers predict very similar intrinsic CCS. This similarity indicates that, despite their contrasting connectivities and levels of N-confusion, all gaseous molecules should display quite similar TWIM drift times particularly in He and N<sub>2</sub> (Fig. 1a). The contrasting ring structures of the N-confused corrole isomers result, however, in contrasting charge dispersions for the protonated molecules as estimated from dipole moment calculations. Ion–molecule complexes with the drift gas of contrasting lifetimes should therefore be formed, and this seems to be the major factor resulting in substantial differences in drift times in CO<sub>2</sub>, a more massive but substantially more polarizable drift gas (Fig. 1b).

### ESI-MS/MS experiments

The ESI-MS/MS data (Fig. 3) for collision induced dissociation (CID) of all protonated isomers demonstrate an interesting sequence of HF losses. Note that substantial rearrangements must be involved prior to the release of these many HF molecules. Although the chemistry is similar, the different structures of such isomers cause pronounced differences in lability.<sup>33</sup> Based on the relative yields of fragments from each precursor ion of *m/z* 797, the lability order for sequential HF loss is corrole < NCC4 < norrole < corrarin < NCC2.

In regard to CID and despite the predominance of HF loss for all isomers, NCC4 was unique being the only isomer in the series to display an extensive loss of NH<sub>3</sub>. Note in Fig. 3d the abundant fragment ion of *m/z* 780. This loss is certainly induced by a unique feature of the NCC4 structure (Scheme 2).

Even though protonation of NCC4 at the 1*H*-pyrrole-like ring (amine, in which the nitrogen atom points away from the core) is

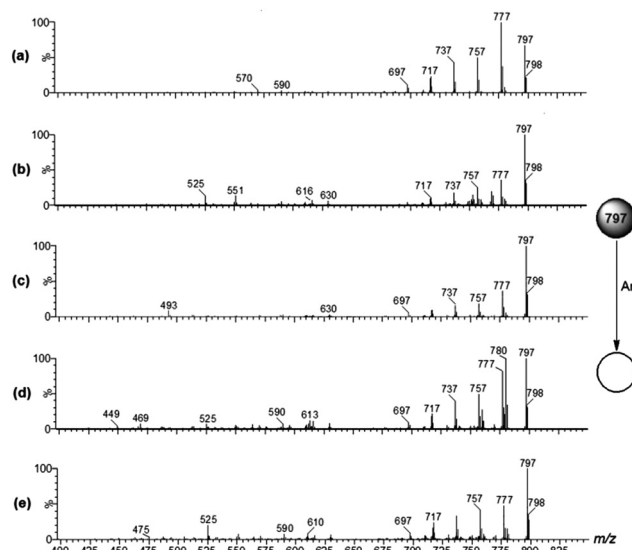


**Fig. 3** ESI-MS/MS for CID of the protonated molecules of (a) corrole, (b) corrarin, (c) NCC2, (d) NCC4 and (e) norrole, using ca. 40 eV of collision energy.

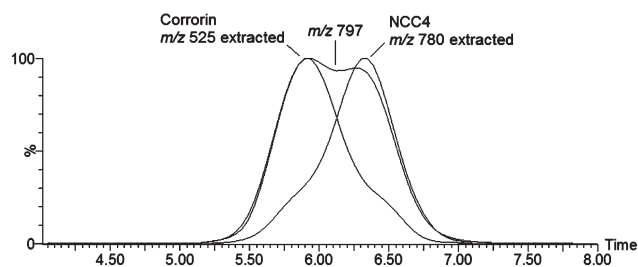


**Fig. 4** Deconvolution of the drift time plot obtained for a mixture of corrarin and NCC4, achieved by extracting individual mobility chromatograms for specific fragment ions: *m/z* 525 for corrarin and *m/z* 780 for NCC4.

less favorable, it can be assumed that isomerization to this species must precede NH<sub>3</sub> loss. From this species, the most accessible pathway to release the energy gained in the CID process is through a rearrangement involving ring opening, hydrogen transfer and, ultimately, elimination of the NH<sub>3</sub> molecule. This behavior is not found for the other isomers probably because of the absence of basic sites in which the nitrogen atom points away from the core. But interestingly, NCC2 also displays a nitrogen atom of the 1*H*-pyrrole-like ring pointing away from the core but fails to lose NH<sub>3</sub> (Fig. 3c). In NCC2, this pyrrole-like ring is surrounded by two C<sub>6</sub>F<sub>5</sub> groups, a structural feature that seems to suppress NH<sub>3</sub> loss, perhaps by hampering H transfer to that specific nitrogen. These results indicate therefore that, among the set of protonated corrole isomers investigated herein, NCC4 is unique displaying in its protonated form a structurally diagnostic loss of NH<sub>3</sub>.

The unique loss of NH<sub>3</sub> for protonated NCC4 seems useful also to improve separations using TWIM-MS with post-TWIM dissociation. Fig. 4 shows the deconvolution of the ion mobility drift plot based on specific fragment ions obtained from a mixture of corrarin and NCC4 in CO<sub>2</sub>. When monitoring the



intact protonated molecule of  $m/z$  797, two broad and nearly unresolved peaks are observed (Fig. 4). But when both isomeric protonated molecules are subjected to CID in the transfer cell in a post-TWIM experiment, and by maintaining fragments time-aligned with their previously separated precursor ions, individual mobility chromatograms for each isomer could be registered for the fragment ions of  $m/z$  780 (NCC4) and  $m/z$  525 (corrorin). This deconvolution resulted in much better resolved peaks with a reasonable  $R_{p-p}$  of ca. 0.6. Such deconvolution *via* post-TWIM CID has been previously used, for example, in the distinction of isomeric peptides.<sup>34,35</sup>

## Conclusions

The structural changes promoted by changing the connectivity of nitrogen and carbon atoms in the corrole ring results in isomers with significant differences in shapes (Fig. 2) but close overall CCS (Table 3). The more pronounced difference is observed for dipole moments for the protonated molecules, and the contrasting charge distributions result in contrasting gas phase mobilities in TWIM cells when using more polarizable drift gases such as CO<sub>2</sub> (Fig. 1). Ion/molecule complexes of variable lifetimes are likely responsible for the significant differences in drift times observed in the TWIM-MS experiments using N<sub>2</sub> and CO<sub>2</sub>, and better resolution between the corrole isomers could be achieved using the more polarizable and massive CO<sub>2</sub> as the drift gas.

Even though they seem to require substantial rearrangements, sequential losses of HF molecules were found to dominate the dissociation chemistry of the protonated molecules of the corrole isomers investigated. But their unique N-confused connectivities caused contrasting labilities towards CID, whereas NCC4 showed a peculiar and structurally diagnostic loss of NH<sub>3</sub>, allowing its prompt differentiation from the other isomers.

## Experimental section

Corrole and other N-confused analogues were synthesized according to previously described procedures and characterized by spectroscopic and theoretical molecular modeling methods.<sup>24</sup> Samples were diluted in methanol (HPLC grade, Honeywell Burdick & Jackson, MI, USA) with 0.1% (v/v) of formic acid and injected in the spectrometer with a syringe pump. ESI-TWIM-MS experiments were performed using a Waters Synapt HDMS (high definition mass spectrometer, Manchester, UK) mass spectrometer. This instrument, described in detail elsewhere,<sup>36</sup> has a hybrid quadrupole/ion mobility/orthogonal acceleration time-of-flight (*oa*-TOF) geometry. ESI source conditions in the positive ion mode were as follows: capillary voltage 3.0 kV, sample cone 30.0 V, extraction cone 3.0 V, source temperature 100 °C, desolvation temperature 100 °C, desolvation N<sub>2</sub> gas flow rate 400 L h<sup>-1</sup>.

For TWIM separation, the mobility T-wave cell was operated at 2.00 mbar of N<sub>2</sub> or 1.00 mbar of CO<sub>2</sub>, whereas the wave velocity was respectively set at 250 and 280 m s<sup>-1</sup>, and the wave height at 30.0 V. Product ion scan TWIM-MS/MS experiments were performed using  $1.0 \times 10^{-2}$  mbar of argon as collision gas at the transfer cell (after the mobility cell) of the instrument and a collision energy of 40.0 eV. The instrument was previously

calibrated with phosphoric acid oligomers (H<sub>3</sub>PO<sub>4</sub> 0.05% in H<sub>2</sub>O–MeCN 50 : 50 v/v) ranging from  $m/z$  50 to 2000.

Corrole, corrorin, NCC2, NCC4 and norrole structures were optimized, both as neutral and protonated species in each possible basic site, and the respective electronic energies and dipole moments calculated at the B3LYP/6-31G(d,p) level using the Gaussian03 program.<sup>37</sup> The MOLDEN program<sup>38</sup> was used to visualize the results of geometry optimization calculations. Theoretical collision cross sections (CCS) were estimated using the trajectory method (TM) implemented in the MOBCAL software<sup>39</sup> at 298 K. Atomic coordinates and Mulliken charges were extracted from Gaussian03 optimization outputs and inserted into MOBCAL inputs using a PERL script.

## Notes and references

- 1 E. Vogel, M. Köcher, H. Schmickler and J. Lex, *Angew. Chem., Int. Ed. Engl.*, 1986, **25**, 257.
- 2 J. L. Sessler, E. A. Brucker, S. J. Weghorn, M. Kisters, M. Schäfer, J. Lex and E. Vogel, *Angew. Chem., Int. Ed. Engl.*, 1994, **33**, 2308.
- 3 M. A. Aukauloo and R. Guillard, *New J. Chem.*, 1994, **18**, 1205.
- 4 E. Vogel, M. Bröring, S. Weghorn, P. Scholz, R. Deponate, J. Lex, H. Schmickler, K. Schaffner, S. E. Braslavsky, M. Müller, S. Pörting, C. J. Fowler and J. L. Sessler, *Angew. Chem., Int. Ed. Engl.*, 1997, **36**, 1651.
- 5 E. Vogel, M. Bröring, C. Erben, R. Demuth, J. Lex, M. Nendel and K. N. Houk, *Angew. Chem., Int. Ed. Engl.*, 1997, **36**, 353.
- 6 H. Furuta, T. Asano and T. J. Ogawa, *J. Am. Chem. Soc.*, 1994, **116**, 767.
- 7 P. J. Chmielewski, L. Latos-Grażyński, K. Rachlewicz and T. Glowiak, *Angew. Chem., Int. Ed. Engl.*, 1994, **33**, 779.
- 8 T. D. Lash, A. D. Lammer and G. M. Ferrence, *Angew. Chem., Int. Ed.*, 2011, **50**, 9718.
- 9 M. Toganoh and H. J. Furuta, *J. Org. Chem.*, 2010, **75**, 8213.
- 10 D. T. Gryko, *J. Porphyrins Phthalocyanines*, 2008, **12**, 906.
- 11 A. Rebane, M. Drobizhev, N. S. Makarov, B. Kozzarna, M. Tasior and D. T. Gryko, *Chem. Phys. Lett.*, 2008, **462**, 246.
- 12 B. Kozzarna, R. Voloshchuk and D. T. Gryko, *Synthesis–Stuttgart*, 2007, **9**, 1339.
- 13 T. Ding, E. A. Alemán, D. A. Modarelli and C. J. Ziegler, *J. Phys. Chem. A*, 2005, **109**, 7411.
- 14 P. Swider, A. Nowak-Król, R. Voloshchuk, J. P. Lewtak, D. T. Gryko and W. Danikiewicz, *J. Mass Spectrom.*, 2010, **45**, 1443.
- 15 (a) M. R. M. Domingues, P. Domingues, M. G. P. M. S. Neves, A. C. Tomé and J. A. S. Cavaleiro, *J. Porphyrins Phthalocyanines*, 2009, **13**, 524; (b) D. M. Tomazela, F. C. Gozzo, I. Mayer, F. M. Engelmann, K. Araki, H. E. Toma and M. N. Eberlin, *J. Mass Spectrom.*, 2004, **39**, 1161; (c) M. N. Eberlin, K. Araki, A. D. P. Alexiou, A. L. B. Formiga, H. E. Toma, S. Nikolaou and D. M. Tomazela, *Organometallics*, 2006, **25**, 3245; (d) Y. Chan, X. Li, M. Soler, J. L. Wang, C. Wesdemiotis and G. R. Newkome, *J. Am. Chem. Soc.*, 2009, **131**, 16395.
- 16 J. F. B. Barata, C. M. Barros, M. G. O. Santana-Marques, M. G. P. M. S. Neves, M. A. F. Faustino, A. C. Tomé, A. J. F. Correia and J. A. S. Cavaleiro, *J. Mass Spectrom.*, 2007, **42**, 225.
- 17 K. M. Downard, S. D. Maleknia and S. Akashi, *Rapid Commun. Mass Spectrom.*, 2012, **26**, 226.
- 18 D. B. Vieira, A. M. J. Crowell and A. A. Doucette, *Rapid Commun. Mass Spectrom.*, 2012, **26**, 523.
- 19 I. Carames-Pasaron, J. A. Rodríguez-Castrillón, M. Moldovan and J. I. G. Alonso, *Anal. Chem.*, 2012, **84**, 121.
- 20 (a) N. A. Pierson, L. Chen, S. J. Valentine, D. H. Russel and D. E. Clemmer, *J. Am. Chem. Soc.*, 2011, **133**, 13810; (b) T. Wyttenbach and M. T. Bowers, *J. Phys. Chem. B*, 2011, **115**, 12266.
- 21 (a) A. A. Shvartsburg and R. D. Smith, *Anal. Chem.*, 2008, **80**, 9689; (b) S. Shiki, M. Ukibe, Y. Sato, S. Tomita, S. Hayakawa and M. Ohkubo, *J. Mass Spectrom.*, 2008, **43**, 1686; (c) S. D. Pringle, K. Giles, J. L. Wildgoose, J. P. Williams, S. E. Slade, K. Thalassinou, R. H. Bateman, M. T. Bowers and J. Scrivens, *Int. J. Mass Spectrom.*, 2007, **261**, 1; (d) A. A. Shvartsburg and R. D. Smith, *Anal. Chem.*, 2008, **80**, 9689; (e) D. P. Smith, T. W. Knappman, I. Campuzano, R. W. Malham, J. T. Beryman, S. E. Radford and A. E. Ashcroft, *Eur. J. Mass Spectrom.*, 2009, **15**, 113; (f) B. T. Ruotolo, K. Giles, I. Campuzano,

- A. M. Sandercock, R. H. Bateman and C. V. Robinson, *Science*, 2005, **310**, 1658.
- 22 P. M. Lalli, B. A. Iglesias, D. K. Deda, H. E. Toma, G. F. Sá, R. J. Daroda, K. Araki and M. N. Eberlin, *Rapid Commun. Mass Spectrom.*, 2012, **26**, 263.
- 23 P. M. Lalli, B. A. Iglesias, H. T. Toma, G. F. Sa, R. J. Daroda, J. C. Silva, J. E. Szulejko, K. Araki and M. N. Eberlin, *J. Mass Spectrom.*, 2012, **47**, 712.
- 24 K. Fujino, Y. Hirata, Y. Kawabe, T. Morimoto, A. Srinivasan, M. Toganoh, Y. Miseki, A. Kudo and H. Furuta, *Angew. Chem., Int. Ed.*, 2011, **50**, 6855.
- 25 H. Furuta, H. Maeda and A. Osuka, *J. Am. Chem. Soc.*, 2001, **123**, 6435.
- 26 M. Toganoh and H. Furuta, *Chem. Commun.*, 2012, **48**, 937.
- 27 D. P. Smith, T. W. Knapman, I. Campuzano, R. W. Malham, J. T. Berryman, S. E. Radford and A. E. Ashcroft, *Eur. J. Mass Spectrom.*, 2009, **15**(2), 113.
- 28 M. Tabrizchi and F. Rouholahnejad, *Talanta*, 2006, **69**, 87.
- 29 P. M. Lalli, Y. E. Corilo, M. Fasciotti, M. F. Riccio, F. M. Nachtigall, G. F. de Sa, R. J. Daroda, G. H. M. F. Souza, I. Campuzano and M. N. Eberlin, *Anal. Chem.*, 2012, submitted.
- 30 K. Giles, J. P. Williams and I. Campuzano, *Rapid Commun. Mass Spectrom.*, 2011, **25**, 1559.
- 31 G. R. Asbury and H. H. Hill, *Anal. Chem.*, 2000, **72**, 580.
- 32 *The PyMOL Molecular Graphics System, Version 1.4*, Schrödinger, LLC.
- 33 K. S. F. Lau, M. Sadilek, M. Gouterman, G. E. Khalil and C. Brückner, *J. Am. Soc. Mass Spectrom.*, 2006, **17**, 1306.
- 34 I. Riba-Garcia, K. Giles, R. H. Bateman and S. J. Gaskell, *J. Am. Soc. Mass Spectrom.*, 2008, **19**, 608.
- 35 L. F. A. Santos, A. H. Iglesias, A. F. Gomes and F. C. Gozzo, *J. Am. Soc. Mass Spectrom.*, 2010, **21**, 2062–2069.
- 36 (a) K. Giles, S. D. Pringle, K. R. Worthington, D. Little, J. L. Wildgoose and R. H. Bateman, *Rapid Commun. Mass Spectrom.*, 2004, **18**, 2401; (b) S. D. Pringle, K. Giles, J. L. Wildgoose, J. P. Williams, S. E. Slade, K. Thalassinou, R. H. Bateman, M. T. Bowers and J. J. Scrivens, *Int. J. Mass Spectrom.*, 2007, **261**, 1.
- 37 M. J. Frisch, G. W. Trucks, H. B. Schlegel, G. E. Scuseria, M. A. Robb, J. R. Cheeseman, J. A. Montgomery, Jr., T. Vreven, K. N. Kudin, J. C. Burant, J. M. Millam, S. S. Iyengar, J. Tomasi, V. Barone, B. Mennucci, M. Cossi, G. Scalmani, N. Rega, G. A. Petersson, H. Nakatsuji, M. Hada, M. Ehara, K. Toyota, R. Fukuda, J. Hasegawa, M. Ishida, T. Nakajima, Y. Honda, O. Kitao, H. Nakai, M. Klene, X. Li, J. E. Knox, H. P. Hratchian, J. B. Cross, V. Bakken, C. Adamo, J. Jaramillo, R. Gomperts, R. E. Stratmann, O. Yazyev, A. J. Austin, R. Cammi, C. Pomelli, J. W. Ochterski, P. Y. Ayala, K. Morokuma, G. A. Voth, P. Salvador, J. J. Dannenberg, V. G. Zakrzewski, S. Dapprich, A. D. Daniels, M. C. Strain, O. Farkas, D. K. Malick, A. D. Rabuck, K. Raghavachari, J. B. Foresman, J. V. Ortiz, Q. Cui, A. G. Baboul, S. Clifford, J. Cioslowski, B. B. Stefanov, G. Liu, A. Liashenko, P. Piskorz, I. Komaromi, R. L. Martin, D. J. Fox, T. Keith, M. A. Al-Laham, C. Y. Peng, A. Nanayakkara, M. Challacombe, P. M. W. Gill, B. Johnson, W. Chen, M. W. Wong, C. Gonzalez and J. A. Pople, *GAUSSIAN 03 (Revision C.02)*, Gaussian, Inc., Wallingford CT, 2004.
- 38 G. Schaftenaar and J. H. Noordik, *J. Comput. Aided Mol. Des.*, 2000, **14**, 123–134.
- 39 (a) <http://www.indiana.edu/~nano/software.html>; (b) M. F. Mesleh, J. M. Hunter, A. A. Shvartsburg, G. C. Schatz and M. F. Jarrold, *J. Phys. Chem.*, 1996, **100**, 16082–16086; (c) A. A. Shvartsburg and M. F. Jarrold, *Chem. Phys. Lett.*, 1996, **261**, 86.